nature astronomy

ARTICLES

https://doi.org/10.1038/s41550-019-0918-5

Plasma densities near and beyond the heliopause from the Voyager 1 and 2 plasma wave instruments

D. A. Gurnett* and W. S. Kurth

The heliopause is the boundary between the hot heliospheric (solar wind) plasma and the relatively cold interstellar plasma. Pressure balance considerations show that there should be a large (factor of 20 to 50) density increase across the heliopause. Here we report electron density measurements from the Voyager 1 and 2 plasma wave instruments near and beyond the heliopause. The plasma density in the outer heliosphere is typically about 0.002 cm^{-3}. The first electron density measured by the Voyager 2 plasma wave instrument in the interstellar medium, 0.039 cm^{-3} ± 15%, was on 30 January 2019 at a heliocentric radial distance of 119.7 au. The density jump, about a factor of 20, confirms that Voyager 2 crossed the heliopause. The new density is very similar to the first density measured in the interstellar medium by the Voyager 1 plasma wave instrument, 0.055 cm^{-3}, on 23 October 2013 at a radial distance of 122.6 au. These small differences in the densities and radial distances are probably due to the relative locations of the spacecraft in the boundary layer that forms in the interstellar plasma just beyond the heliopause.

After finishing their exploration of the outer planets, the Voyager 1 (V1) and Voyager 2 (V2) spacecraft, launched in 1977, were sent on a new mission to reach the heliopause, which is the boundary[1–4] between the hot, >10^5 K, plasma in the outer heliosphere[5] and the relatively cold, 10^4 K, plasma in the very local interstellar medium (VLISM)[6]. The spacecraft were then both moving outward toward the 'nose' of the heliopause[7,8], with V1 moving north relative to the ecliptic plane and V2 moving south (Fig. 1). V1 reached the heliopause[9–12] on 25 August 2012 at a heliocentric radial distance of 121.6 au, and as reported in this issue V2 tentatively reached the heliopause[13–16] on 5 November 2018 at a heliocentric radial distance of 119.0 au. Because the plasma instrument[17] (PLS) on V1 failed in 1980, and the comparable PLS instrument on V2 is only marginally able to determine the plasma density[16] in the VLISM, the V1 and V2 plasma wave instruments (PWS)[18] have played a key role in determining the plasma density in the region near and beyond the heliopause.

The PWS uses a V-shaped electric dipole antenna with an effective length of 7 m to detect the electric field of waves in the surrounding plasma. When a shock wave from the Sun propagates into the interstellar plasma it produces an electron beam ahead of the shock that drives electron plasma oscillations at the local electron plasma frequency via a beam-plasma instability[19]. The electron density can then be computed from the frequency of the plasma oscillations[20], which is given by

$$f_p = 8{,}980\sqrt{n_e}\ \text{Hz} \quad (1)$$

where n_e is the local electron number density per cubic centimetre. Such shock-related plasma oscillations can also produce radio emissions via nonlinear wave–wave interactions and are known to be the source of type II solar radio emissions in the solar wind[21], and heliospheric 2–3 kHz radio emissions in the interstellar medium[22].

V1 observations

First, we concentrate on the description and analysis of the V1 plasma wave observations. An example of the electric-field waveform of electron plasma oscillations detected by V1 ahead of an interstellar shock[19] is shown in the top panel of Fig. 2, with the corresponding electric-field spectrum in the bottom panel. Note the very sharp peak in the spectrum produced by the electron plasma oscillation at $f_p = 2.65$ kHz. Using equation (1) for the electron plasma oscillation frequency, the local electron density in this case is 0.0871 cm^{-3}. It is obvious from the sharp peak in the spectrum that such electron plasma oscillations can give very accurate measurements of the local electron density. However, in any specific case there are sometimes fluctuations and sideband effects[12] that can reduce the accuracy of the electron density measurements. On the relatively long timescales used in this Article (minutes to hours), the accuracy of the electron density measurements obtained from the wideband waveform measurements is typically of the order of plus or minus a few per cent.

Next, we give an overview of the fairly extensive electron density measurements available in the interstellar medium from the V1 PWS wideband data. The frequencies of plasma oscillations observed by V1 are conveniently displayed by plotting the electric-field spectra in the form of a colour-coded frequency–time spectrogram as shown in the top panel of Fig. 3. Over the nearly seven years since V1 crossed the heliopause, a total of eight clearly defined plasma oscillation events have been identified. The electron density associated with each of these events can be determined from the scale on the right-hand side of the frequency–time spectrogram. As can be seen, the detailed structures of the plasma oscillations vary considerably, from fairly narrow well defined emissions, such as during the October–November 2012 event[23], to much more complex emissions, such as during the February–November 2014 event[19]. However, there is a clearly defined increase in the interstellar plasma density with increasing radial distance from the heliopause.

Department of Physics and Astronomy, University of Iowa, Iowa City, IA, USA. *e-mail: donald-gurnett@uiowa.edu

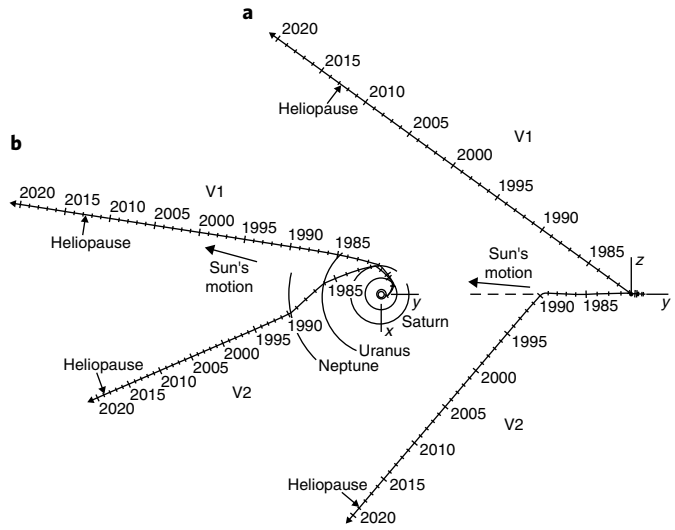

Fig. 1 | Trajectories of V1 and V2 in inertial (*x*, *y*, *z*) ecliptic coordinates. **a**, Projection onto the *y*–*z* plane. **b**, projection onto the *x*–*y* plane. The time is in years, starting with launch in 1977, and the locations of the V1 and V2 crossings of the heliopause are indicated.

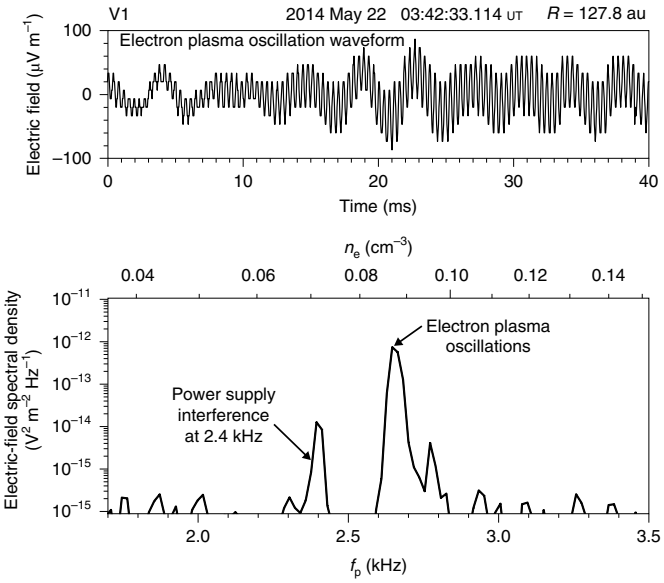

Fig. 2 | Typical electric-field waveforms of electron plasma oscillations and their associated electric-field power spectrum as detected by V1. These electric-field waveforms were obtained from the PWS wideband receiver just ahead of a shock[19] that occurred on 24 August 2014. *R*, heliocentric radial distance. Note the very sharp peak in the electric-field power spectrum produced by the plasma oscillations at $f_p = 2.65$ kHz. The corresponding electron density, as obtained from the equation $f_p = 8{,}980\sqrt{n_e}$ Hz, is 0.0871 cm^{-3}. The peak at 2.40 kHz is due to interference from the spacecraft 2.40 kHz power supply.

Specifically, the electron density increased from about 0.055 cm^{-3} near the heliopause at 122.6 au to about 0.12 cm^{-3} in the most recent data at 146 au, a region that we shall call the 'boundary layer' in the VLISM. This systematic increase matches almost perfectly with the density ramp inferred from the frequency–time spectra of transient 2–3 kHz heliospheric radio emissions observed by V1 and V2 more than 25 years ago[22]. The origin of the boundary layer that forms in the VLISM just beyond the heliopause remains uncertain, although several plausible mechanisms have been suggested. These include a plasma 'pileup effect' in the interstellar plasma flow around the nose of the heliosphere[22,24], an interaction with the 'neutral hydrogen wall' that forms near the heliopause[25] and a 'plasma depletion layer' produced by an anisotropy-driven instability upstream of the heliosphere[26]. The pileup model suggests that a peak should eventually be reached in the radial density profile, and the slight decline in the plasma frequency from the May–June 2018 event to the recent May–June 2019 event suggests that V1 may have reached this peak.

To relate the plasma oscillation events to interstellar shocks, the bottom panel shows the magnetic-field strength from the V1 magnetometer (Fig. 3). The two black vertical dashed lines labelled 'Shock' identify jumps in the magnetic-field strength that are known to be caused by shock waves from the Sun propagating outward through the interstellar plasma. The first[23] is clearly associated with the October–November 2012 plasma oscillation event, and the second[19] is clearly associated with the February–November 2014 plasma oscillation event. These two events provide the most convincing evidence that the plasma oscillations are caused by low-energy electron beams propagating ahead of interstellar shocks originating from the Sun, just as for type II solar radio bursts[21]. However, because of energy and sensitivity limitations of the energetic charged particle detectors on Voyager we have not been able to detect the electron beams that are driving the plasma oscillations. As for the electron plasma oscillation events that do not have a clear shock signature in the magnetic field, we believe that they are produced by magnetic-field-aligned electron beams from distant shocks that have not passed close enough to Voyager to be detected by the magnetometer.

V2 observations

Having described the interstellar plasma densities determined from the V1 PWS we next turn to the recent V2 PWS measurements. Because the plasma density measurement technique relies on the presence of shocks to drive the plasma oscillations, we cannot rely on the existence of the PWS electron density measurements at any given time. This was indeed the case when the Cosmic Ray[13], Low Energy Charged Particle[14], Magnetometer[15] and PLS[16] instruments on V2 detected the characteristic signatures of the heliopause on 5 November 2018. No plasma oscillations were detected by the PWS at that time because there was no suitable shock of solar origin propagating outward from the Sun. However, nearly three months later, on 30 January 2019, electron plasma oscillations began to be detected (Fig. 4) in the 1.78 kHz channel of the 16-channel PWS spectrum analyser. This frequency channel corresponds to an electron density of 0.039 cm^{-3}. Note that there is no evidence of plasma oscillations in the adjacent 1.00 and 3.11 kHz channels, so the oscillation frequency must be near 1.78 kHz. See Supplementary Information for our best estimate of the error limits on the corresponding electron density, which are 0.039 cm^{-3} ± 15%. The plasma oscillations continued with their characteristic spiky intensity variations until about 25 February 2019, where they abruptly disappeared. According to the usual sequence of events, when the upstream plasma oscillations end, the causative shock should be observed[19]. In fact, there is an unusual jump in the PLS current around this time[16] (J. D. Richardson, personal communication). However, we cannot confirm that this jump is associated with a shock because the calibrated magnetic-field data for this time period are not currently available.

V1 and V2 comparisons

We next compare the heliocentric radial variations of the plasma densities observed by V1 and V2 (Fig. 5). The filled black circles are electron densities obtained from the V1 plasma oscillation measurements, starting near the solar wind termination shock (TS) at 94.0 au (black circles with error bars)[27] in the lower left-hand corner, and

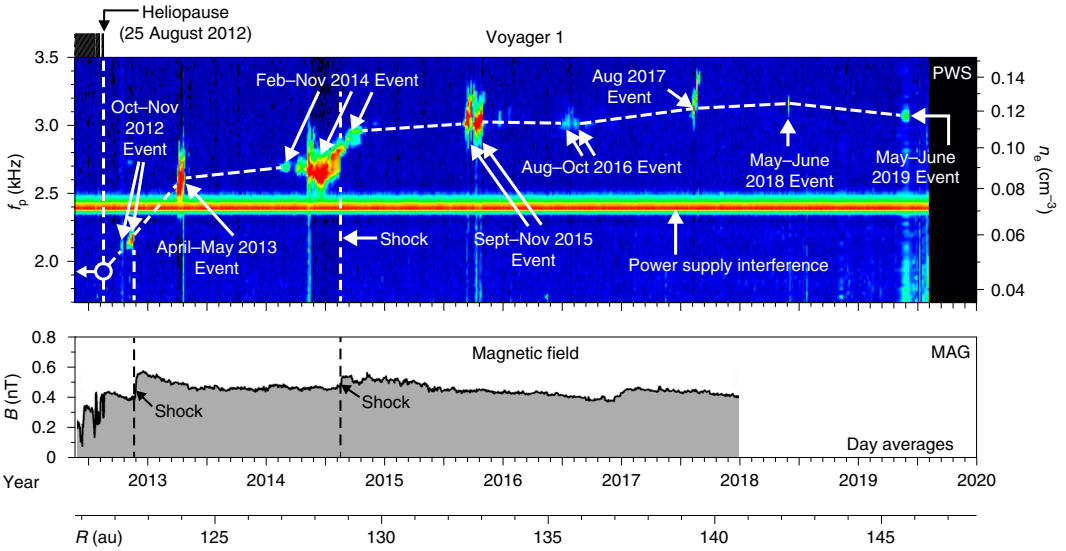

Fig. 3 | Frequency–time spectrogram of electron plasma oscillations detected by the V1 PWS wideband receiver, and the corresponding local magnetic-field strength from the magnetometer. The electric-field intensity is indicated by the colour, with red being the most intense and blue being the least intense. The electron density corresponding to the oscillation frequencies is given by the scale on the right-hand side of the spectrogram. The jumps in the magnetic-field strength indicated by the two vertical dashed lines are shocks that have propagated outward into the interstellar medium from coronal mass ejections at the Sun.

ending with the most recent V1 plasma oscillation measurements at 146 au in the upper right-hand corner. The horizontal dashed black line starting at 90 au with a density of about 0.0012 cm^{-3}, continuing to the near-vertical jump at 122.6 au, is an interpolation of the V1 PWS electron densities. This interpolation is based on the expectation[12] that the density in the very hot heliosheath plasma would remain nearly constant until the spacecraft reaches the heliopause (HP), after which it should jump upward by a large factor due to the entry into the much colder interstellar plasma.

The filled red circles are the comparable plasma densities obtained from the V2 PWS and PLS instruments (Fig. 5). The first two measurements in the bottom left-hand corner (red circles with error bars) are electron densities obtained from plasma oscillations detected by the PWS 16-channel spectrum analyser near the V2 termination shock[28] at about 83.7 au. The next series of red circles (with no error bars) is the proton densities obtained from the V2 PLS instrument[29], which end with a density of 0.0044 cm^{-3} at 118.9 au on 26 October 2018. The next red circle (with error bars) at the end of the near-vertical red dashed line is the electron density, 0.039 cm^{-3} ± 15%, obtained at 119.7 au from the previously described plasma oscillations in the 1.78 kHz channel (Fig. 4).

Given that the electron and proton number densities should be nearly the same in the proton-dominated plasma in the outer heliosphere and interstellar medium, the radial dependences of the plasma number densities obtained from V1 and V2 (black and red circles) are strikingly similar, almost identical in overall shape and detail. The close similarity is especially remarkable given the substantially different spacecraft trajectories, and the different phases of the solar cycle in which the observations were made. However, we do note that the difference in the heliospheric radial distance of the V1 and V2 termination shock (TS) crossings, 10.3 au, is significantly larger than the corresponding difference in the radial distance of the heliopause (HP) crossings, 2.6 au (Fig. 5). This lack of proportionality relative to the distance from the Sun suggests that either solar cycle variations in the solar wind pressure[30] or north–south asymmetries in the interstellar magnetic-field pressure[31] are playing some role in affecting the relative locations of

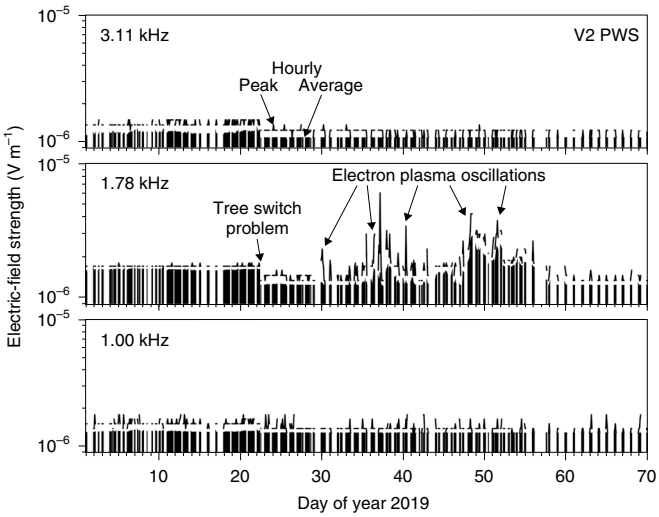

Fig. 4 | Three panel plots of the electric-field intensities from the V2 PWS 16-channel spectrum analyser. The spiky highly irregular signals with large peak-to-average intensity ratios in the 1.78 kHz channel are electron plasma oscillations. Note that the plasma oscillations are not observed in the adjacent 1.00 kHz and 3.11 kHz channels, which means that the oscillation frequency must be near 1.78 kHz. High-frequency–time-resolution spectrograms, such as in Fig. 3, which give much better frequency resolution, are not available from the V2 PWS because of a failure in the wideband receiver several years ago. The abrupt irregular steps that occasionally occur in the instrument noise level, such as the one marked 'Tree switch problem', are due to a failure in the V2 data system a few months after launch.

the termination shock and the heliopause. Also, although the location of the first V2 PWS density measurement at 119.7 au (R_2) is controlled by the arrival time of the shock that excited the plasma oscillations, this density point, together with the last V2 PLS density measurement at 118.9 au (R_1), can be viewed as putting a

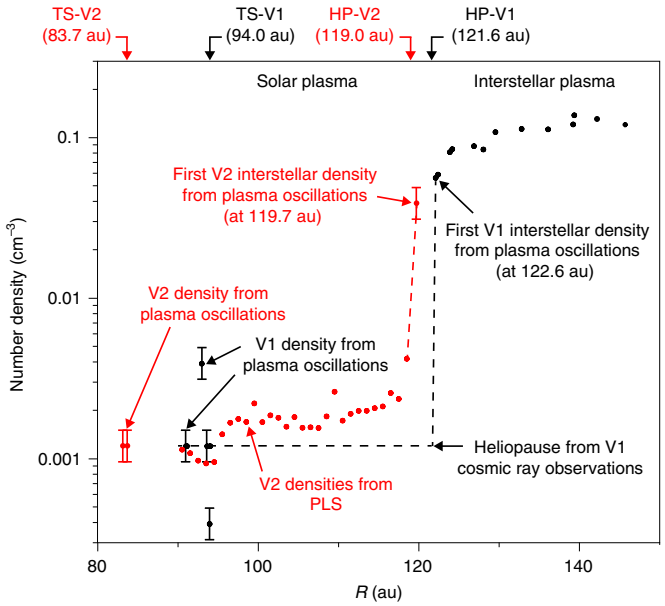

Fig. 5 | Comparison of the plasma number densities measured by V1 and V2. The filled black circles are the electron densities determined from the V1 PWS, and the red circles are densities (1 au averages) determined from the V2 PWS and PLS instruments. The PWS measures electron number densities and the PLS measures proton number densities, which are expected to be nearly the same in the proton-dominated heliospheric and interstellar plasmas. Error bars for the V2 PWS densities in the interstellar medium are ±15%; see the discussion in Supplementary Information. The heliocentric radial density variations observed by the two spacecraft are strikingly similar, especially given their very different north–south trajectories (Fig. 1) and the different phases of the solar cycle during which the observations were obtained.

lower limit on the steepness of the plasma density gradient near the heliopause,

$$\begin{aligned}\Delta n/\Delta R &= (n_{R_2} - n_{R_1})/(R_2 - R_1)\\ &> (0.0390 - 0.0044)\,\mathrm{cm^{-3}}/(119.7 - 118.9)\,\mathrm{au}\\ &= 0.043\,\mathrm{cm^{-3}\,au^{-1}}\end{aligned}$$

Conclusions

The V1 and V2 detections of electron plasma oscillations triggered by shocks propagating outward from the Sun have played a key role in determining the radial variation of the plasma density in the outer heliosphere and in the nearby interstellar medium. The extensive V1 electron density measurements show the existence of a relatively thick boundary layer with a scale thickness of 10 au or more, which extends beyond the heliopause into the VLISM with an asymptotic (possibly peak) electron density of about 0.12 cm^{-3}. The recent first V2 PWS density measurement in the VLISM, 0.039 cm^{-3}, is in very close agreement with the densities first measured by the V1 PWS when it entered the VLISM, 0.055 cm^{-3}, and occurred at almost the same heliospheric radial distance, 119.7 au versus 122.6 au. These measurements, the exact timing of which is controlled by shocks arriving from the Sun, occurred just slightly beyond the heliopause, 119.0 au versus 121.6 au, as detected by the other instruments on V1 and V2. The resulting radial density profile obtained from both spacecraft (Fig. 5) provides striking confirmation of the boundary layer that exists in the VLISM near the nose of the heliosphere, as first inferred from V1 and V2 remote radio measurements of a density ramp at the nose of the heliosphere over 25 years ago[22].

As far as future observations are concerned, it remains to be seen whether V1 will remain operational long enough to determine whether the interstellar plasma density has reached a peak, as suggested by Fig. 3, or is now at an asymptotic level characteristic of the local interstellar medium. Nor do we know if V2 will remain operational long enough to confirm the 10 au scale size of the boundary layer in the VLISM that is so notably evident in the V1 PWS electron density measurements. Also, it will be interesting to see if there is a distance limit beyond which electron plasma oscillations are no longer produced due to the progressive weakening of shocks as they propagate farther from the Sun into the interstellar medium.

Methods

The Voyager instruments (PWS) consist of two major components, (1) a wideband receiver that provides 4 bit high-time-resolution electric-field waveforms at a sample rate of 28,800 samples s^{-1} and (2) a 16-channel (10 Hz to 56 kHz) spectrum analyser that provides low-rate samples of the electric-field spectrum (four channels per decade) at a rate that is currently one spectrum every 16 s. Since the data from the wideband waveform receiver have a bit rate much too high to be transmitted in real time, they are stored on the spacecraft digital tape recorder for later transmission at a much lower bit rate. Normally, one 48 s sample of the wideband waveform data is taken once per week, and the data are stored on the spacecraft tape recorder and played back once every four months. The exact pattern of waveform data collection can be reprogrammed by ground command and has changed considerably over the course of the mission. Due to a failure in the V2 PWS wideband receiver a few years ago, high-time-resolution wideband data are no longer available from the V2 spacecraft.

Data from the 16-channel PWS spectrum analyser are transmitted in real time. Whether the spectrum analyser data are recorded on the ground depends on the availability of a ground receiving antenna at one of the three NASA Deep Space Network tracking stations. Typically, 8–12 h of such real-time data are available per day for each spacecraft, although the coverage can vary greatly from day to day depending on competition from other spacecraft missions. A failure in the V2 spacecraft data system shortly after launch (the tree switch failure indicated in Fig. 4) has led to abrupt unpredictable shifts in the instrument noise level that makes these data difficult to analyse.

Once the tape-recorded and real-time data are received by the NASA Deep Space Network, they are sent via a satellite link to the Jet Propulsion Laboratory in Pasadena, CA, where the data for each instrument are stripped out of the data stream and forwarded for analysis to the responsible institution. In the case of the PWS, the data are processed at the University of Iowa to check for errors in the data transmission, to make plots of the types presented in this Article and to put the data in the proper format for archiving in the NASA Planetary Data System and the Space Physics Data Facility.

Data availability

The data used in this paper are archived on an approximately annual basis in the Planetary Data System (https://pds.nasa.gov) and can also be found in the Space Physics Data Facility at https://cdaweb.gsfc.nasa.gov/misc/NotesV.html#VG2_PWS_LR (V2) or https://cdaweb.gsfc.nasa.gov/misc/NotesV.html#VG1_PWS_LR (V1).

Received: 5 July 2019; Accepted: 16 September 2019;
Published online: 04 November 2019

References

1. Davis, L. E. Jr. Interplanetary magnetic fields and cosmic rays. *Phys. Rev.* **100**, 1440–1444 (1955).
2. Parker, E. N. *Interplanetary Dynamical Processes* (Interscience, 1963).
3. Axford, W. I. Introductory lecture—The heliosphere. In *Physics of the Outer Heliosphere: Proc. 1st COSPAR Colloq. held in Warsaw, Poland, 19–22 September 1989* (eds Grzedzielski, S. & Page, D. E.) 7–15 (Pergamon, 1990).
4. Zank, G. P. Faltering steps into the galaxy: the boundary regions of the heliosphere. *Annu. Rev. Astron. Astrophys.* **53**, 449–500 (2015).
5. McComas, D. J. et al. IBEX observations of heliospheric energetic neutral atoms: current understanding and future direction. *Geophys. Res. Lett.* **38**, L18101 (2011).
6. Frisch, P. C., Redfield, S. & Slavin, J. D. The interstellar medium surrounding the Sun. *Annu. Rev. Astron. Astrophys.* **49**, 237–279 (2011).
7. Zank, G. P. Interaction of the solar wind with the local interstellar medium: theoretical perspective. *Space Sci. Rev.* **89**, 413–688 (1999).
8. Ajello, J. M., Stewart, A. I., Thomas, G. E. & Garps, A. Solar cycle study of interplanetary Lyman-alpha variations: Pioneer Venus Orbiter sky background results. *Astrophys. J.* **317**, 964–968 (1987).
9. Stone, E. C. et al. Voyager 1 observes low energy galactic cosmic rays in a new region depleted of heliospheric ions. *Science* **341**, 150–153 (2013).

10. Krimigis, S. M. et al. Search for the exit: Voyager 1 at heliosphere's border with the galaxy. *Science* **341**, 141–147 (2013).
11. Burlaga, L. F., Ness, N. F. & Stone, E. C. Magnetic field observations as Voyager 1 enters the heliosheath depletion region. *Science* **341**, 147–150 (2013).
12. Gurnett, D. A., Kurth, W. S., Burlaga, L. F. & Ness, N. F. In situ observations of interstellar plasma with Voyager 1. *Science* **341**, 1489–1492 (2013).
13. Stone, E. C., Cummings, A. C., Heikkila, B. C. & Lal, N. Cosmic ray measurements from Voyager 2 as it crossed into interstellar space. *Nat. Astron*. https://doi.org/10.1038/s41550-019-0928-3 (2019).
14. Krimigis, S. M. et al. Energetic charged particle measurements from Voyager 2 at the heliopause and beyond. *Nat. Astron*. https://doi.org/10.1038/s41550-019-0927-4 (2019).
15. Burlaga, L. F. et al. Magnetic field and particle measurements made by Voyager 2 at and near the heliopause. *Nat. Astron*. https://doi.org/10.1038/s41550-019-0920-y (2019).
16. Richardson, J. D., Belcher, J. W., Garcia-Galindo, P. & Burlaga, L. F. Voyager 2 plasma observations of the heliopause and interstellar medium. *Nat. Astron*. https://doi.org/10.1038/s41550-019-0929-2 (2019).
17. Bridge, H. S. et al. The plasma experiment on the 1977 Voyager mission. *Space Sci. Rev.* **21**, 259–287 (1977).
18. Scarf, F. L. & Gurnett, D. A. A plasma wave investigation for the Voyager mission. *Space Sci. Rev.* **21**, 289–308 (1977).
19. Gurnett, D. A. et al. Precursors to interstellar shocks of solar origin. *Astrophys. J.* **809**, 121 (2015).
20. Gurnett, D. A. & Bhattacharjee, A. *Introduction to Plasma Physics* 2nd edn, 10 (Cambridge Univ. Press, 2017).
21. Bale, S. D. et al. The source region of an interplanetary type II radio burst. *Geophys. Res. Lett.* **26**, 1573–1576 (1999).
22. Gurnett, D. A., Kurth, W. S., Allendorf, S. C. & Poynter, R. L. Radio emission from the heliopause triggered by an interplanetary shock. *Science* **262**, 199–203 (1993).
23. Burlaga, L. F., Ness, N. F., Gurnett, D. A. & Kurth, W. S. Evidence for a shock in interstellar plasma: *Voyager 1*. *Astrophys. J. Lett.* **778**, L3 (2013).
24. Steinolfson, R. S., Pizzo, V. J. & Holzer, T. Gasdynamic models of the solar wind/interstellar medium interaction. *Geophys. Res. Lett.* **21**, 245–248 (1994).
25. Baranov, V. B. & Malama, Yu. G. Model of the solar wind interaction with the local interstellar medium: numerical solution of the self-consistent problem. *J. Geophys. Res.* **98**, 157–163 (1993).
26. Fuselier, S. A. & Cairns, I. H. The 2-3 kHz heliospheric radiation, the *IBEX* ribbon, and the three-dimensional shape of the heliopause. *Astrophys. J.* **771**, 83 (2013).
27. Gurnett, D. A. & Kurth, W. S. Electron plasma oscillations upstream of the solar wind termination shock. *Science* **309**, 2015–2027 (2005).
28. Gurnett, D. A. & Kurth, W. S. Intense plasma waves at and near the solar wind termination shock. *Nature* **454**, 78–80 (2008).
29. Richardson, J. *VOYAGER 2 Data up Through October 26, 2018* (MIT Space Plasma Group, 2018); http://web.mit.edu/afs/athena/org/s/space/www/voyager/voyager_data/voyager_data.html; ftp://space.mit.edu/pub/plasma/vgr/v2/ha/key
30. Washimi, H., Tanaka, T. & Zank, G. P. Time-varying heliospheric distance to the heliopause. *Astrophys. J. Lett.* **846**, L9 (2017).
31. Pogorelov, N., Heerikhuisen, J. & Zank, G. P. Probing heliospheric asymmetries with an MHD-kinetic model. *Astrophys. J.* **675**, L41–L44 (2008).

Acknowledgements

The authors thank J. Richardson and L. Burlaga for providing unpublished PLS and magnetometer data. The research at the University of Iowa was supported by NASA through contract 1622510 with the Jet Propulsion Laboratory.

Author contributions

D.A.G. is the Principal Investigator of the Voyager PWS investigation and W.S.K. the Co-Investigator. D.A.G. is responsible for the overall conduct of the investigation and wrote the initial draft of the paper. W.S.K. is responsible for the data processing and initial identification of the events discussed in the paper and has contributed comments and corrections to the paper.

Competing interests

The authors declare no competing interests.

Additional information

Supplementary information is available for this paper at https://doi.org/10.1038/s41550-019-0918-5.

Correspondence and requests for materials should be addressed to D.A.G.

Peer review information *Nature Astronomy* thanks Stephen Fuselier, G. P. Zank and the other, anonymous, reviewer(s) for their contribution to the peer review of this work.

Reprints and permissions information is available at www.nature.com/reprints.

Publisher's note Springer Nature remains neutral with regard to jurisdictional claims in published maps and institutional affiliations.